

Supporting Information for

An interpenetrating network poly(diethylene glycol carbonate) based polymer electrolyte towards solid state lithium batteries

Xiaochen Liu,^{ab} Guoliang Ding,^b Xinhong Zhou,^{* a} Shizhen Li,^{ab} Weisheng He,^{ab} Jingchao Chai,^b Chunguang Pang,^b Zhihong Liu^{* b} and Guanglei Cui^{* b}

*a. College of Chemistry and Molecular Engineering, Qingdao University of Science & Technology, Qingdao 266042, China. *E-mail: zxhhx2008@163.com.*

*b. Qingdao Industrial Energy Storage Research Institute, Qingdao Institute of Bioenergy and Bioprocess Technology, Chinese Academy of Sciences, Qingdao 266101, China. *E-mail: liuzh@qibebt.ac.cn, cui gl@qibebt.ac.cn; Tel: +86-532-80662746.*

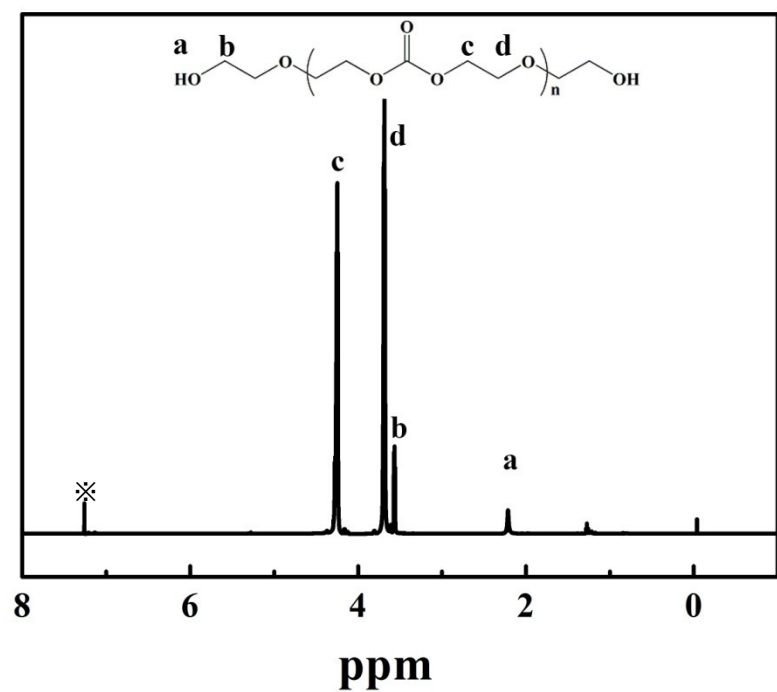


Fig. S1. ^1H NMR spectra of PDEC in CDCl_3 .

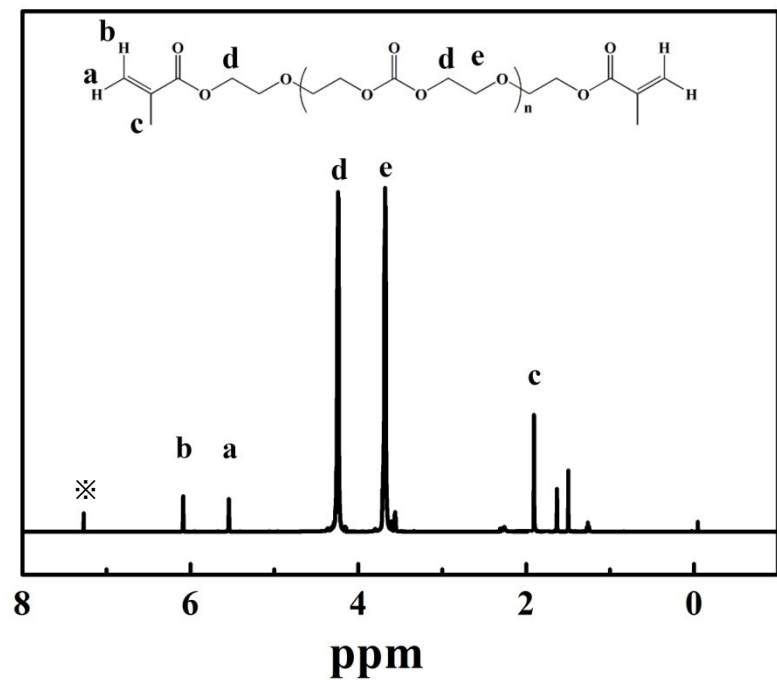


Fig. S2. ^1H NMR spectra of PDEC-DMA in CDCl_3 .

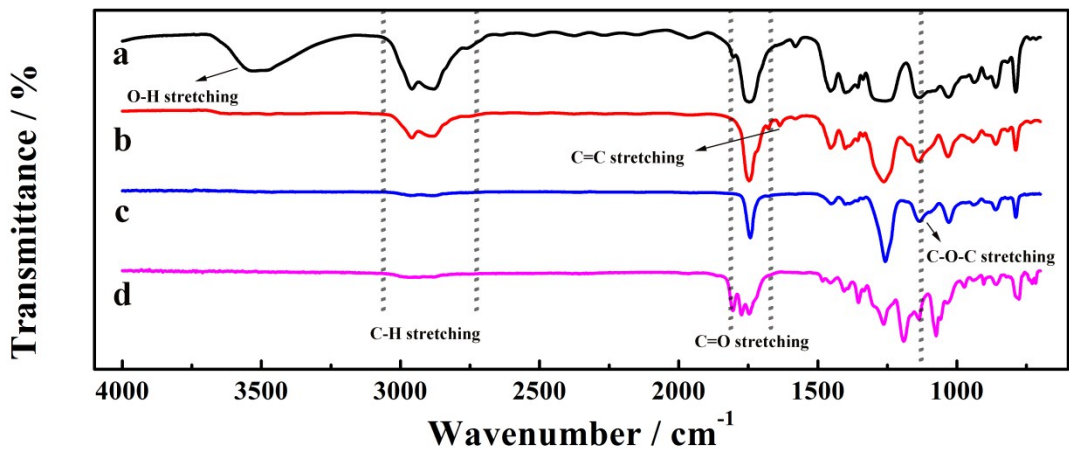


Fig. S3. FTIR spectra of (a) PDEC, (b) PDEC-DMA; ATR-FTIR spectra of (c) IPN-PDEC, (d) IPN-PDEC-LiTFSI₂₀.

Tab. S1. Analysis of FT-IR spectrum

Wavenumber / cm ⁻¹	Analysis
3535	stretching vibration of hydroxyl
2872-2872	stretching vibration of C-H
1756	stretching vibration of C=O from carbonate and methacrylate
1634	stretching vibration of C=C from methacrylate
1396-1456	bending vibration of CH ₂
1259	stretching vibration of C-O from carbonate and methacrylate
1128	stretching vibration of C-O-C from ether
786	bending vibration of O=C-O from carbonate

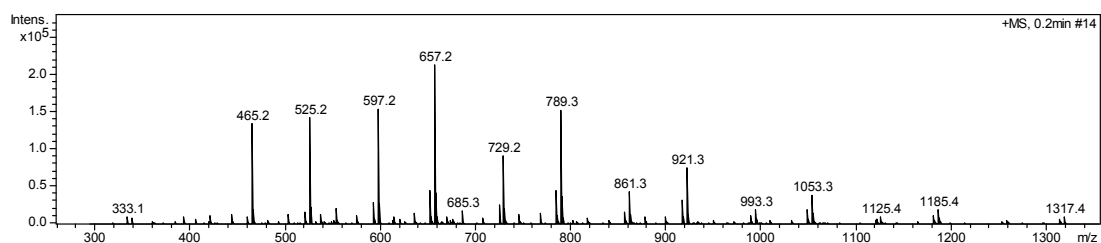


Fig. S4. ESI-MS distribution of PDEC.

Tab. S2. ESI-MS data analysis of PDEC.

Type I :								
n	2	3	4	5	6	7	8	9
m/z	393	525	657	789	921	1053	1185	1317
Type II:								
n	2	3	4	5	6	7	8	9
m/z	333	465	597	729	861	993	1125	1257

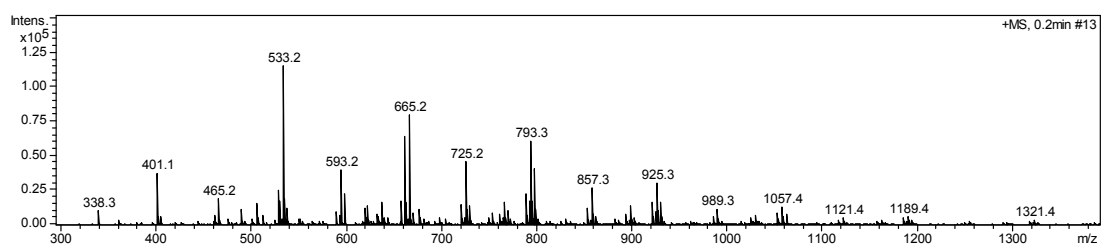


Fig. S5. ESI-MS distribution of PDEC-DMA.

Tab. S3. ESI-MS data analysis of PDEC-DMA.

Type I :						
n	2	2	4	5	6	
m/z	401	533	665	797	929	
Type II:						
n	2	3	4	5	6	7
m/z	461	593	725	857	989	1121
Type III:						
n	2	3	4	5		
m/z	528	661	793	925		

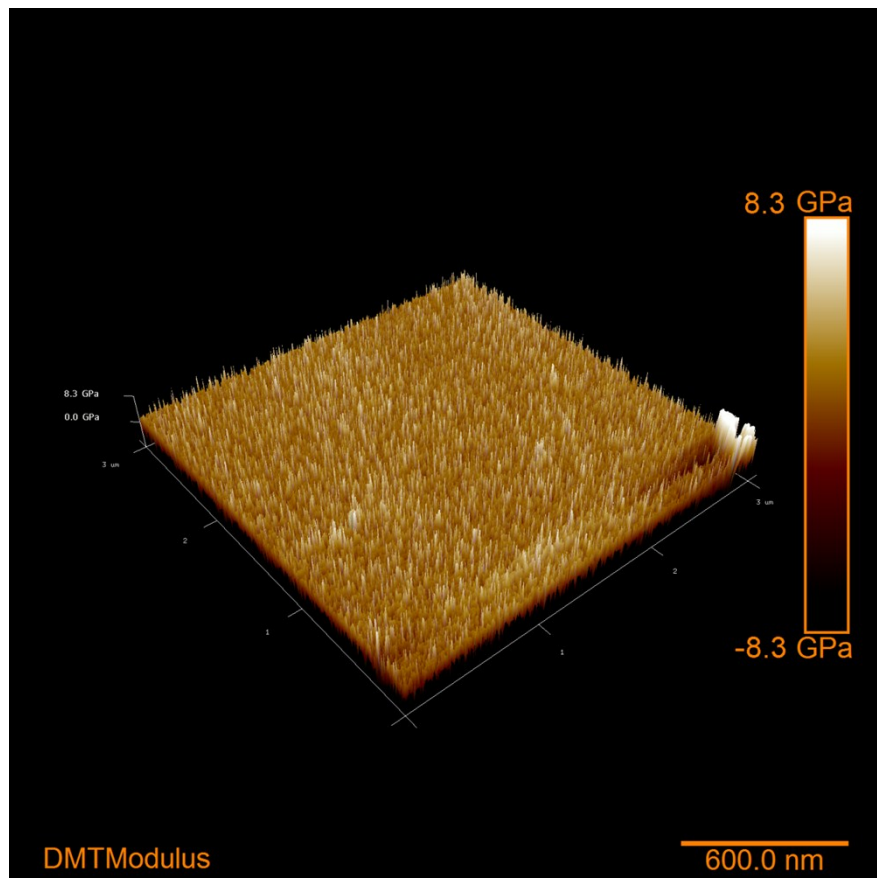


Fig. S6. Young' modulus mapping of the IPN-PDEC.

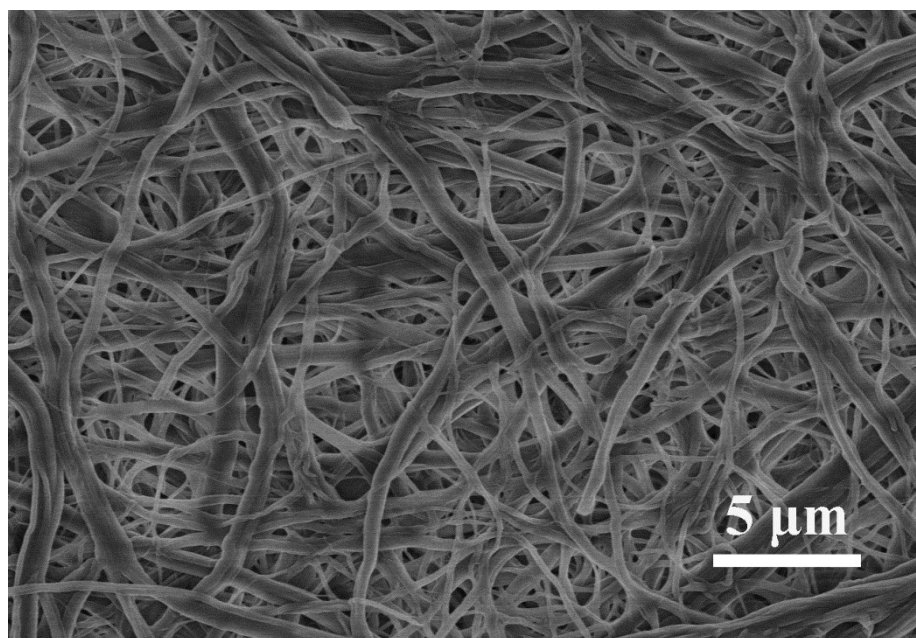


Fig. S7. The SEM image of pristine cellulose.

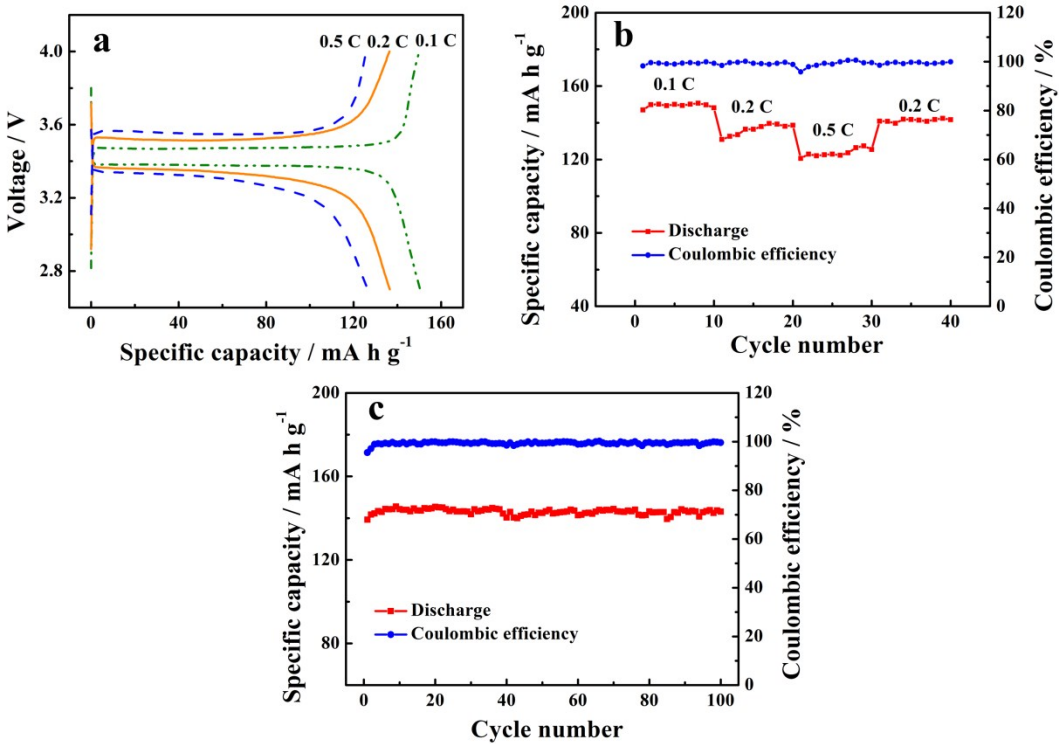


Fig. S8. (a) The charge/discharge profiles and (b) C-rate capability of LiFePO₄/IPN-PDEC-LiTFSI₂₀/Li cells with varied C-rates at 25 °C; (c) cycling performance of LiFePO₄/IPN-PDEC-LiTFSI₂₀/Li cells at a charge/discharge current intensity of 0.2 C and cut-off voltage of 2.75V to 4.0 V at 25 °C.

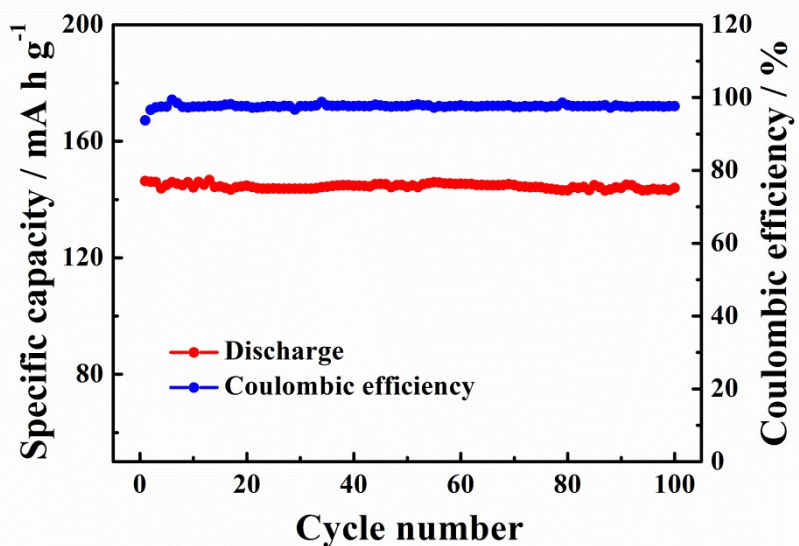


Fig. S9. The cycling performance of Li/cellulose+(1 M LiTFSI+EC/DMC)/LiFePO₄ at a charge/discharge current intensity of 0.2 C and cut-off voltage of 2.75V to 4.0 V at 25 °C.

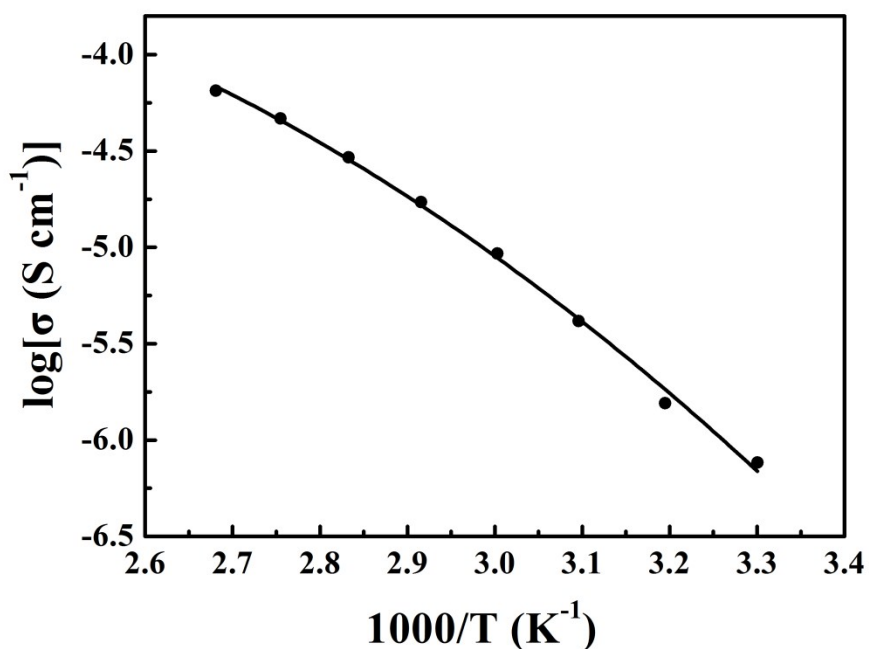


Fig. S10. Temperature of dependence of ionic conductivity of SPE-PDEC-LiTFSI₂₀.

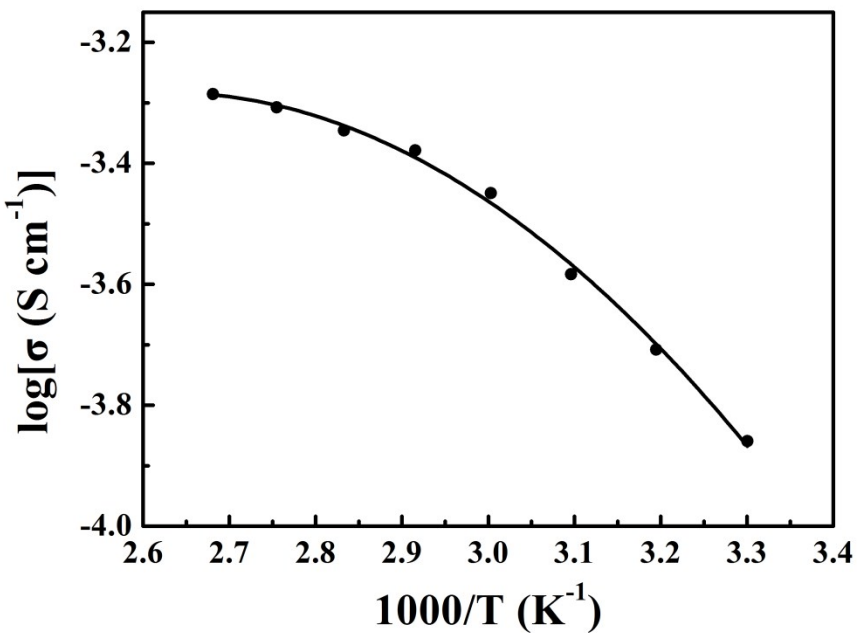


Fig. S11. Temperature dependence of ionic conductivity of IPN-PDEC-LiDFOB₁₅.